AIP Journal of Applied Physics

Attenuation, absorption, and scattering in silver halide crystals and fibers in the mid-infrared

S. Israeli and A. Katzir

Citation: Journal of Applied Physics **115**, 023104 (2014); doi: 10.1063/1.4861407
View online: http://dx.doi.org/10.1063/1.4861407
View Table of Contents: http://scitation.aip.org/content/aip/journal/jap/115/2?ver=pdfcov
Published by the AIP Publishing

JOURNAL OF APPLIED PHYSICS **115**, 023104 (2014)

Attenuation, absorption, and scattering in silver halide crystals and fibers in the mid-infrared

S. Israeli[a)] and A. Katzir
Raymond and Beverly Sackler Faculty of Exact Science, School of Physics and Astronomy, Tel-Aviv University, Tel-Aviv 69978, Israel

(Received 9 November 2013; accepted 20 December 2013; published online 10 January 2014)

The attenuation and the absorption of silver halide crystal and fibers in the mid-IR were measured. The absorption coefficients of silver halide crystals, deformed crystals, and fibers were measured by laser calorimetry at several different wavelengths in the near-IR and the mid-IR. The absorption coefficients of the fibers were higher than those of the deformed crystals and these were higher than those of the un-deformed crystals. We suggest that the absorption behavior is best described by a weak absorption tail. The total attenuation in fibers was measured using the cut back method. The scattering values were calculated by subtracting the absorption coefficients from the total attenuation coefficients. The scattering in the silver halide fibers was ascribed to pores of estimated size of 0.7 μm. We showed that the main contribution to the attenuation of fibers in the mid-IR range was due to scattering and suggested that reducing the scattering will dramatically improve the transmission of silver halide fibers in the mid-IR. *© 2014 AIP Publishing LLC*.
[http://dx.doi.org/10.1063/1.4861407]

I. INTRODUCTION

Single crystals of silver halides, $AgCl_xBr_{1-x}$ $(0 < x < 1)$, are highly transparent from the ultraviolet to the middle-infrared (mid-IR). These crystals may be extruded through small dies to form fibers that are transparent in the mid-IR, typically in the spectral range of 5–20 μm. Fibers of typical diameters 0.7–0.9 mm and lengths of several meters are flexible, non-toxic, and non-hygroscopic. Because of their unique optical and mechanical properties, these fibers have been used in many different applications such as IR radiometry, mid-IR spectroscopy, high power laser delivery, sensors for environmental protection, and biomedical applications.[1] The transmission of silver halide crystals and fibers is limited by Urbach absorption[1] in the visible range and by multiphonon absorption[1] in the far infrared. The theoretical prediction is that the crystals and the fibers should have extremely low losses in the mid-IR.

In the past, the absorption coefficients of such single crystals and fibers were measured at $\lambda = 10.6\,\mu$m by laser calorimetry[2] and the total attenuation of the fibers was measured by the cut-back technique in the mid-IR range. The absorption coefficients of $AgCl_xBr_{1-x}$ crystals and fibers at this wavelength were found to depend[2] on the Cl concentration. In addition, a peak in the absorption coefficient was measured[3] in the fibers at $\lambda \sim 9.7\,\mu$m. This peak does not exist in single crystals of silver halides. But, experimentally the measured attenuation was much higher than the theoretical prediction. This indicates that both the absorption and the scattering are probably higher than expected. The cause for the higher absorption in the mid-IR range in silver halide crystals and fibers is yet un-known.

During the past few years, several explanations for the absorption in the mid-IR were suggested. Multiphonon absorption,[4] absorption by free charge carriers,[5] absorption by cation vacancies localized at charged dislocations,[2,3] and intraband absorption by free holes in the valence band[6] have all been proposed as explanations for the absorption in AgClBr crystals and fibers in the mid-IR. The bulk scattering in these fibers is known to follow the λ^{-2} law in the infrared range, instead of the expected λ^{-4} Rayleigh law. This indicates that the bulk scattering is due to some scattering mechanism that had not yet been identified. The main reason for scattering has been usually attributed to fluctuations of the index of refraction in grains or pores inside the fiber core.[4] Butvina *et al.*[7] were the first to suggest that the main scattering in AgClBr fibers is due to microscopic pores in the fiber core. Sa'ar and Katzir[8] measured the scattering intensity along the fiber length. They found that there were places along the fiber where the scattered power increased sharply. The excess scattering in these "hot spots" was a result of defects or cracks in the fiber surface. Sliberstein *et al.* suggested, using a mode diffusion theory,[9] that in silver halide fibers the scattering in the core increases the cone angle of the beam emerging from the fiber, and surface scattering decreases the cone angle and both dictate the far field distribution. All these authors concluded that the main scattering mechanism in silver halide fibers is core scattering. Bunimovich *et al.*[10] annealed silver halide fibers at different temperatures and showed that grain size increased with annealing temperature. This led to undesirable deterioration of the mechanical properties, and therefore the annealing experiments were not pursued.

In this work, we measured the absorption of silver halide crystals, deformed crystals, and extruded fibers by laser calorimetry at several wavelengths in the near-IR and the mid-IR spectral ranges. We then measured the attenuation of silver

---

[a)] saritisrae@walla.com

halide fibers by the cut-back technique. By subtracting the absorption from the attenuation, we were able to obtain more detailed information about the scattering in the fibers.

The importance of this work is that it provides independent information about the absorption and the scattering in the silver halide fibers. This will undoubtedly help in finding techniques for improving the transmission of the fibers hence improve the performance of these fibers in the various applications.

II. EXPERIMENTAL TECHNIQUES

The following paragraph describes the experimental techniques used for absorption and attenuation measurements.

A. Absorption technique

The absorption coefficients of many crystals in the near-IR and mid-IR are very low. At present, the thermometric laser calorimetry is the most widely used technique for the determination of the optical absorption coefficients of such highly transparent materials.[11,12] In this case, the sample is placed inside an insulated chamber, which is often evacuated. A laser beam is transmitted through the sample, and the increase in temperature is monitored as a function of time, using a thin thermocouple that is attached to the sample. One technique uses continuous wave (CW) laser calorimetry, and there are actually two variations of this technique: isothermic[13] and adiabatic.[11,14] In the isothermal technique, the sample is heated by a CW laser beam till it reaches a steady state temperature. Then the laser is turned off and the temperature decay rate is measured. The absorption coefficient is calculated from temperature increase ΔT_0 in the steady state, with respect to the temperature of the environment, the temperature decay rate τ, and the incident laser power P_0. The absorption coefficient α_{abs} is described by the following equation:

$$\alpha_{abs} = \frac{CA\Delta T_0}{\tau P_0}, \tag{1}$$

where A is the cross section of a sample with a cylindrical shape and P_0 is the incident laser power. It should be noted that in case of isothermal technique only the total absorption coefficient α_{abs} can be determined.

In the adiabatic technique, the sample is heated by the CW laser radiation and the temperature is measured as a function of time. For $\alpha_{abs}L \ll 1$, we can calculate α_{abs} as follows:

$$\alpha_{abs} L P_T = \frac{2n}{n^2+1} mc \left(\frac{dT}{dt}\bigg|_{heating} + \frac{dT}{dt}\bigg|_{cooling} \right), \tag{2}$$

where m is the sample mass, c is the specific heat, n is the index of refraction, and P_T is the power transmitted through the sample. This expression is valid if the thermal diffusivity is large and the heat losses are small.

The absorption coefficient measured by the adiabatic method is also the total absorption coefficient α_{abs}. It can be separated into two contributions: the bulk absorption coefficient α_b and the surface absorption coefficient α_s

$$\alpha_{abs} L = \alpha_b L + 2\alpha_s, \tag{3}$$

where L is the sample length. The most direct way of separating α_b and α_s is by measuring $\alpha_{abs}L$ as a function of L. Then, the slope of the graph is α_b and the intercept on the L axis is $2\alpha_s$.

Another method for determining α_b and α_s is to use the adiabatic calorimetric technique on a sample shaped like a long rod. The thermocouple is placed at the center of the sample and the transit time due to the surface absorption is smaller than the transit time due to the bulk absorption. Therefore, the heating profile of the rod will have two slopes, the initial slope of the heating curve will be due to bulk absorption and the final slope will be due to the total absorption.[2]

The pulsed calorimetric technique is very similar to the CW laser calorimetric techniques, mentioned above. But, instead of using a continuous laser beam, one uses a high energy short laser pulse.[15,16] The common method, used by many researchers, was the CW calorimetric technique, but some investigators also used the pulsed calorimetric method. For example, Nistor *et al.*[15,16] described CO_2 laser pulsed calorimetry of a KCl rod in a vacuum chamber. They compared[15] the results of the pulsed and CW calorimetry techniques and showed that the value calculated from the pulsed results was close to the value of the bulk absorption, calculated from the CW results. These authors explained their results by the fact that the time required for the heat to reach from the long rod surfaces to the center of the rod (i.e., the measurement point) was much smaller than the pulse duration. Bagdasarov *et al.*[17] and Zhekov *et al.*[18] showed the dependence of the absorption coefficients on the pulse length. When using short pulses ($t < 1\,\mu s$), these authors observed nonlinear effects. They[18] suggested that the nonlinear effects were due to defects with large local absorption coefficients. In such a case, the relationship between the length of the laser pulse and the time scale of the heat transfer between the crystal and the particle should be taken into account.

In the linear time regime, the absorption coefficient is calculated as follows:

$$\alpha_{abs} L = \frac{2n}{n^2+1} \frac{mc\Delta T}{E}, \tag{4}$$

where E is the output energy and ΔT is the temperature increase. It should be noticed that in this case the power densities used for heating the samples are very high and the samples should withstand the operating conditions, without being damaged.

B. Attenuation and scattering techniques

The attenuation of silver halide fibers in the infrared is composed of scattering and absorption, and the total attenuation coefficient is given by the following equation:

$$\alpha_{tot}(\lambda) = \alpha_{abs}(\lambda) + \alpha_{sca}(\lambda), \tag{5}$$

where α_{tot} is the total attenuation coefficient, α_{abs} is the total absorption coefficient, and α_{sca} is the scattering coefficient.

The total attenuation coefficient in the infrared is normally measured by the cut-back technique.[19] This technique involves measurements of the transmission of a fiber of length L, then gradually cutting off segments of the fiber and measuring the transmission of shorter lengths of the same fiber. This set of measurements gives more accurate value of the attenuation coefficient of the fiber. The attenuation coefficient α_{tot} in cm^{-1} can be calculated by the following equation:

$$\alpha_{tot} = \frac{1}{(L_2 - L_1)} \ln\left(\frac{P_{L_2}}{P_{L_1}}\right), \tag{6}$$

where P_{L_1} is the fiber transmission of fiber length L_1 and P_{L_2} is the fiber transmission of fiber length L_2. This process can be repeated several times. The cut-back technique allowed us to disregard the Fresnel reflections from the two end faces, which are canceled out in Eq. (6). In this case, it is assumed that the fiber is homogeneous, i.e., it is assumed that the attenuation coefficient along the fiber is constant.

The scattering coefficient can be calculated from Eq. (4), after that the total attenuation and the absorption coefficient are measured.

1. Scatterers

The scatterers' type and size can be calculated using the Mie theory and some numerical calculations. In a previous research,[20] we showed that the bulk scattering in silver halide fibers is mainly due to pores, as had also been suggested previously by Butvina *et al.*[7] It was shown there[20] that the scattering coefficient can be described by the following equation:

$$\alpha_s \propto N_s \frac{\langle a\rangle^{\eta+2}}{\lambda^{\eta}}, \tag{7}$$

where N_s is the number of scatterers per unit volume, $\langle a\rangle$ is the average radius of the scatterers, assuming that all the scatterers are spherical, that λ is the wavelength and that the power coefficient η is in the range of 0–4. The value of η can be calculated from the experimental results and by using few more numerical calculations, assuming the scatterers are pores, one can estimate the size of scatterers. Such an analysis will be more accurate if it will use the η value from the scattering curve, instead of the η value from the attenuation curve, especially if the scatterers are pores.

III. EXPERIMENTAL DETAILS

A. Absorption measurements

Various single crystals, deformed crystals, and extruded fibers were studied, using the experimental set up shown in Figure 1. The same setup was used both for adiabatic, isothermal CW and pulsed laser calorimetry. For crystal measurements, the laser radiation was focused on the middle of the calorimeter, using a long focal length lens. For fiber measurements, we used a short focal length lens, focusing the laser radiation on the input end surface of the fiber. We used ZnSe lenses for CO_2, Ho:YAG, and Nd:YAG lasers and a BK7 lenses for GaAs laser. The absorbed radiation in samples generated temperature increase that was measured by a Copper-Constantan differential thermocouple and a nano-voltmeter (Keithley, Model 181).

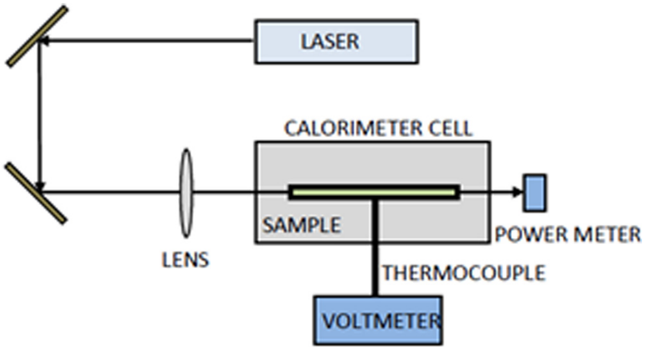

FIG. 1. Schematic drawing of the laser calorimetry measurement setup.

One thermocouple junction was attached to the center of the sample and the second junction was attached to a thermal mass of constant temperature. The power or energy transmitted through the sample was measured by a power-meter (OPHIR, Model 30A). The results of the absorption coefficients measurements of crystals and fibers for each wavelength were statistically analyzed.

1. Measurements on $AgCl_{0.3}Br_{0.7}$ crystals and fibers

a. Pure crystals. Ten pure and homogenous $AgCl_{0.3}Br_{0.7}$ crystals of diameter 7.6 mm and length of several centimeters were grown in our laboratory. The end faces of each crystal were mechanically polished to an optical quality level. The crystals were measured by the adiabatic[2] laser calorimetric technique[11,13,14,21] at three different wavelengths: 10.6 μm, 1.3 μm, and 0.83 μm using three different lasers; CO_2(Apollo, Model 580), Nd:YAG (Quantronix, Model 117), and GaAs (Sharplan, Model 6040), respectively.

b. Fibers extruded from crystals. The above mentioned crystals were extruded through a small die to form optical fibers of diameter 0.9 mm and several meters long. A segment of 10 cm was cut from each long fiber and its end faces were polished. The fiber segments were measured by the isothermal[2] laser calorimetric technique at wavelengths 10.6 μm, 1.3 μm, and 0.83 μm using the same lasers as noted above. The fiber segments were also measured by the pulse laser calorimetric technique[15,16] at the wavelength 2.094 μm, using a Ho:YAG laser (Sharplan, model 2021).

2. Measurements on AgBr crystals and fibers

a. Un-deformed and deformed crystals. Other pure and homogenous AgBr crystals were grown in our laboratory by the Bridgman-Stockbarger technique. The crystals of diameter 7.6 mm and length of several centimeters were polished by the same method as noted before. The crystals were measured by adiabatic laser calorimetry with the same apparatus that had been mentioned above, at wavelengths of 0.83, 1.3, and 10.6 μm. The crystals were then plastically deformed by slow motion of a ram. The plastic deformation level was defined as the relative longitudinal shrinking of the crystal ΔL/L. The crystals were plastically deformed to a level of 8.7%, then their end faces were mechanically polished and they were measured again by the adiabatic calorimetry technique.

b. *Fibers extruded from deformed crystals*. The deformed crystals were extruded to long fibers of diameter 0.9 mm and segments of 10 cm were cut from the long fibers. Their end faces were optically polished and they were measured by isothermal laser calorimetry, as described above at wavelengths of 0.83, 1.3, and 10.6 μm.

B. Attenuation measurements

An un-deformed single crystal of composition $AgCl_{0.3}Br_{0.7}$ was used in these measurements. A disk of thickness of 5 mm was cut from this crystal and its normalized attenuation in the visible and NIR was measured by a visible spectrometer (Jascow Model V-530). Then a fiber of diameter 0.9 mm was extruded from the crystal and its total attenuation coefficient in the mid-IR was measured by the cut-back technique, using an FTIR spectrometer (Bruker, vector 22), as shown in Figure 2.

IV. EXPERIMENTAL RESULTS

A. Absorption and attenuation coefficients

The absorption coefficients of all ten $AgCl_{0.3}Br_{0.7}$ crystals and the fibers extruded from them were statistically analyzed. For each wavelength, the average value was calculated and the error was determined by the spread of the measurement results around the average value. The results of the absorption coefficients measurements (and the statistical error) on $AgCl_{0.3}Br_{0.7}$ crystals and fibers are shown in Figure 3. The absorption coefficients of the fibers were higher than the absorption coefficients of crystals over the entire mid-IR range. Both the absorption of the crystals and of the fibers decreased at longer wavelengths. The absorption coefficients of the un-deformed AgBr crystals, the deformed AgBr crystals, and the fibers extruded from the deformed crystals were measured and the results are shown in Figure 4. The absorption coefficients of the un-deformed crystals had the lowest values over the entire mid-IR range. The absorption coefficients of the deformed crystals were higher than the absorption coefficients of the crystals, as shown in previous research,[22] and the absorption coefficients of the fibers were even higher.

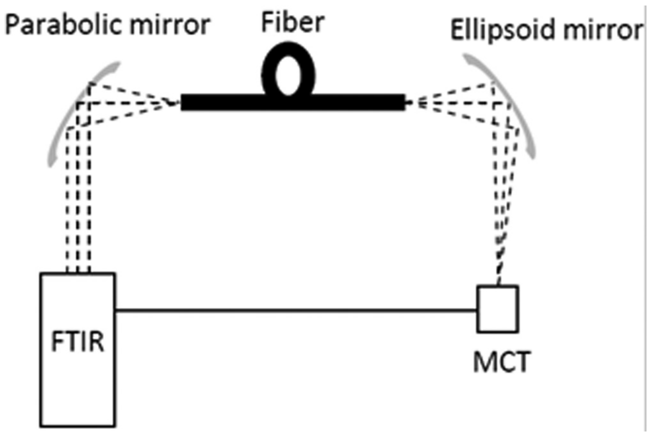

FIG. 2. Schematic drawing of the cut-back setup.

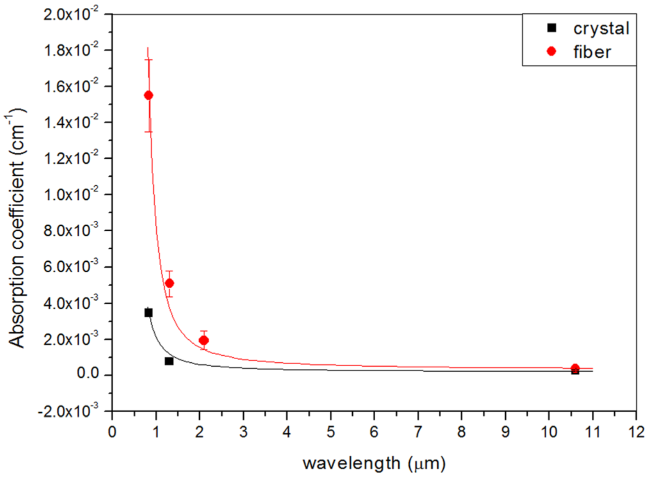

FIG. 3. The absorption coefficients of $AgCl_{0.3}Br_{0.7}$ crystals and fibers.

The absorption coefficients of all the samples decreased at longer wavelengths, similar to the case of the $AgCl_{0.3}Br_{0.7}$ crystals and fibers.

The absorption of one of the $AgCl_{0.3}Br_{0.7}$ extruded fibers was measured by calorimetric technique, and the results are presented in Figure 4 (squares). The graph shows the same behavior as in Figure 3, i.e., the absorption coefficient decreased at longer wavelengths. The total atteuation of this fiber was also measured by the cutback method, and the results are also shown in Figure 5 (solid line). The sharp peaks in the figure are due to H_2O, CO_2, and contamination due to organic conpounds. These peaks are not associated with the samples themselves.[23]

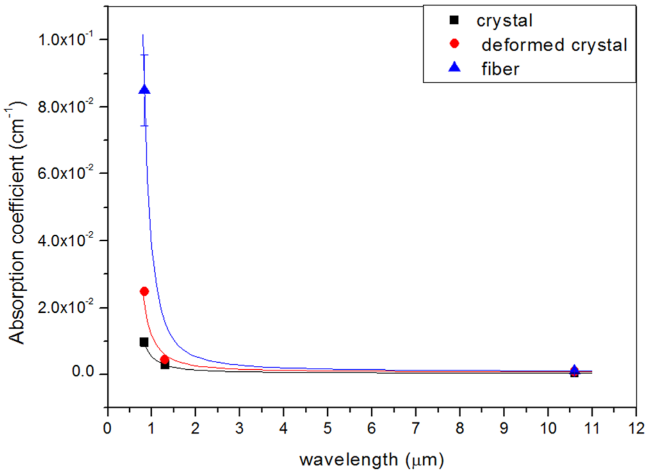

FIG. 4. The absorption coeffiecents of an un-deformed AgBr crystal, a deformed crystal with ΔL/L = 8.7% and of a fiber extruded from the deformed crystal.

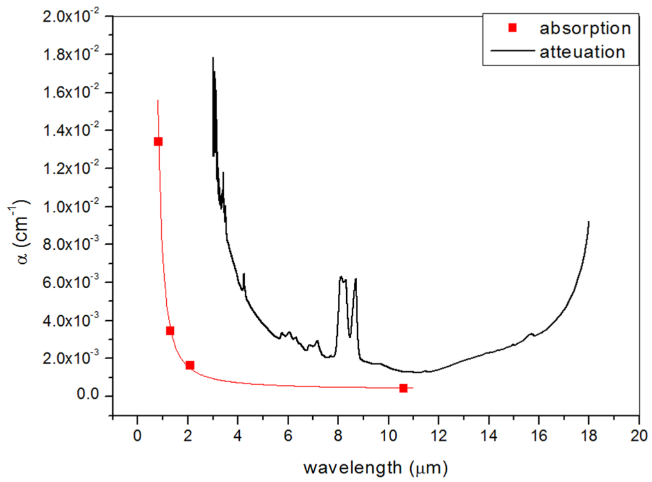

FIG. 5. The absorption coeffiecients of $AgCl_{0.3}Br_{0.7}$ fiber in the mid-IR range measured by the calorimetric techniqueand and the atteuation coeffiecient of this fiber measured by the cutback method.

The normalized loss of $AgCl_{0.3}Br_{0.7}$ crystal disk was measured by the spectrometer in the spectral range 0.45–1.1 μm, and the results are shown in Figure 6. Two different slopes are clearly seen in this graph: there is a very sharp decrease at wavelengths shorter than $\sim$0.48 μm, asscribed to the Urbach absorption, and at longer wavelengths there is a dramatic decrease of the slope.

V. ANALYSIS OF THE RESULTS

A. Absorption coefficient

The absorption coefficient, α_{tot}^{abs}, measured by the calorimetric technique on a cylindrical sample, is the sum of α_b, the absorption of the bulk material and α_s, the absorption of the surfaces of a cylinder[2] of length L. It may be expressed by the following equation:

$$\alpha_{tot}^{abs} = \alpha_b + \frac{2\alpha_s}{L}. \tag{8}$$

Using the adiabatic calorimetry technique for a long cylindrical shape allows a separation of the bulk and the surface absorption coefficients, due to the different arrival times of the bulk and the surface temperature rise to the thermocouple.[14] The initial temperature increase slope is due to bulk absorption and the second slope is due to the total absorption. Also, in order to separate between the coefficients, the scattering intensities should be small. At short wavelengths, the scattering intensities are too high, so it obscures the bulk absorption initial temperature increase. The scattering intensity is low enough only in the case of a long cylindrical crystal and at the wavelength of 10.6 μm. As a result, at shorter wavelengths, only the total absorption coefficient can be measured. In the fiber, due to the large ratio between its length and its diameter, the surface absorption is negligible and the measured absorption represents the bulk absorption[2] coefficient. The absorption measurements of both the $AgCl_{0.3}Br_{0.7}$ crystals and the fibers and of the AgBr crystals, deformed crystals, and fibers showed a decrease of the absorption when the wavelength increased. Although we carried out only several measurements of the absorption in the mid-IR, we assume a continuity of the absorption coefficients over the entire mid-IR range. As mentioned earlier, researches have already offered several explanations for the absorption in the mid-IR range such as multiphonon absorption,[4] absorption by free charge carriers,[5] absorption by cation vacancies localized at charged dislocations,[2,3] and intraband absorption by free holes in the valence band.[6] Urbach and multiphonon absorption extrapolation to the mid-IR range cannot explain the current and past[2] measured absorption coefficients values. Absorption by free carries describes an increase of the absorption when the wavelength is increased, which is in contradiction with our present measurements. Other authors explained the presence of a peak[3] at $\sim$9.7 μm but not the spectral behavior of the absorption in the entire mid-IR range. In addition to the wavelengths dependence, the absorption of the deformed crystals and the absorption of the fibers were higher than those of the un-deformed crystals, as shown in Figures 3 and 4. During crystal deformation and the fiber extrusion, the deformation level was increased and the samples had higher concentration of defects. A possible explanation for our absorption results can be the weak absorption tail (WAT), which had been demonstrated mainly in glasses[24,25] but also measured in several crystalline materials.[26] WAT appears as a continuation to the Urbach tail[1] at longer wavelengths and is attributed to defects, disorder, and impurities. Its spectral behavior is similar to the Urbach spectral behavior but with different parameters. Equation (9) describes the spectral dependence of the WAT

$$\alpha = \alpha_0 \exp\left(\frac{hc}{E_0} * \frac{1}{\lambda}\right), \tag{9}$$

where α is the absorption coefficient, h is Planck constant, c is the speed of light, λ is the wavelength, and α_0 and E_0 are parameters of the material. Changing the equation to its logarithm form will give a linear dependence of α in $1/\lambda$:

$$\ln \alpha = \ln \alpha_0 + \frac{hc}{E_0} * \frac{1}{\lambda}. \tag{10}$$

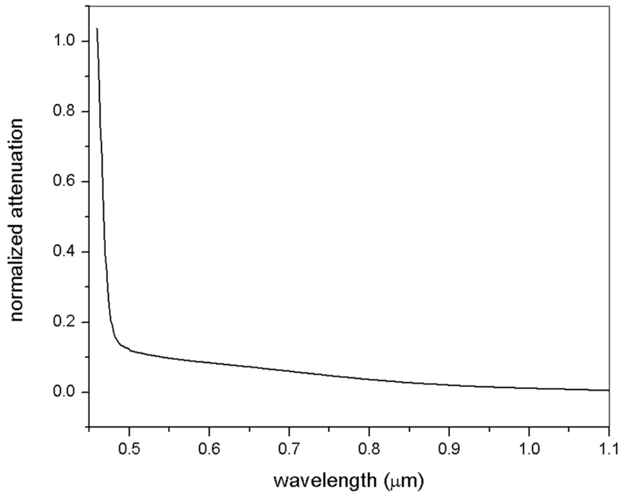

FIG. 6. The normalized losses of $AgCl_{0.3}Br_{0.7}$ crystal at low wavelength range.

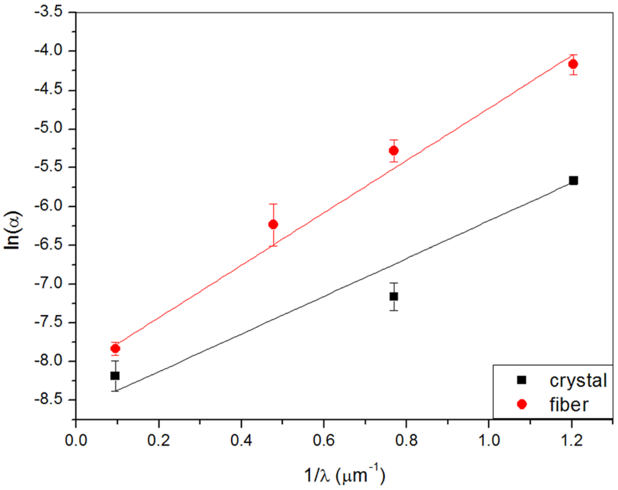

FIG. 7. $AgCl_{0.3}Br_{0.7}$ crystals and fibers dependence in $1/\lambda$.

In order to check the idea that WAT is responsible for some of our experimental results, we plotted the absorption as a function of $1/\lambda$. Figure 7 shows the dependence of the logarithm of the absorption on $1/\lambda$ for the $AgCl_{0.3}Br_{0.7}$ crystals and for the fibers extruded from them. Figure 8 shows similar results for the AgBr crystals, the deformed crystals, and the fibers extruded from them.

We indeed found a linear dependence of $\ln(\alpha)$ on $1/\lambda$. Using Eq. (10), we calculated the activation energy E_0 for each sample, as shown in Table I.

The activation energy, E_0, was in the range of 0.3–0.5 eV and it seems that the fibers had smaller activation energies than crystals. The above values are in the same energy range as was found by Hidefumi *et al.*[26] for other crystals and amorphous materials, such as KRS-6, KCl, CsI, LiF, and SiO_2.

TABLE I. The calculated activation energy E_0 of the different samples.

		E_0 (eV)
$AgCl_{0.3}Br_{0.7}$	Crystal	0.51
	Fiber	0.37
AgBr	Crystal	0.45
	Deformed crystal	0.42
	Fiber	0.32

B. Attenuation and scattering coefficients

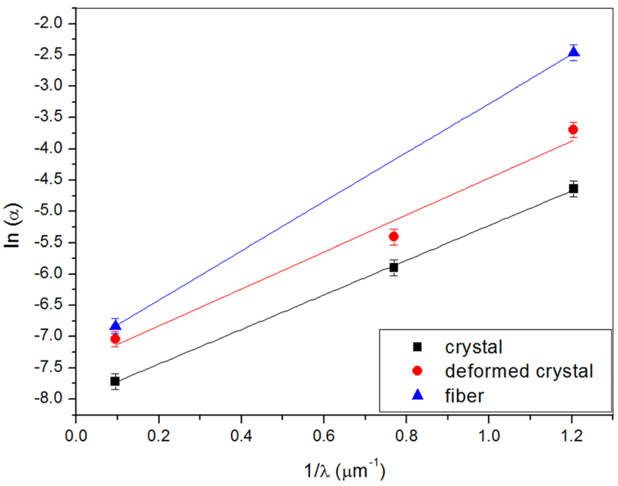

FIG. 8. AgBr crystals, deformed crystals, and fibers dependence in $1/\lambda$.

The attenuation coefficient, α_{tot}, is the sum of the absorption coefficient α_{tot}^{abs} and of the scattering coefficient $\alpha_{sca.}$ as indicated in Eq. (5). Figure 5 shows the measured attenuation coefficient and the measured absorption coefficient of the $AgCl_{0.3}Br_{0.7}$ fiber. We calculated the continuous spectral absorption curve according to Eq. (9), based on the measured absorption data, and the parameters found in linear fit of Eq. (10). We subtracted the absorption coefficient curve from the attenuation coefficient curve and thus isolated the wavelength dependence of the scattering coefficient only, as shown in Figure 9.

Based on this graph, the ratio of the scattering coefficient to the total attenuation coefficient at different wavelengths was calculated. It can be seen that the attenuation in this range is mostly composed of scattering. The scattering constitutes 95% of the attenuation at the wavelength 3 μm and 65% of the attenuation at the wavelength 10.6 μm. The scattering in fibers is ascribed to fluctuation of the index of refraction due to grains, pores,[20] or voids,[1,4] and is described by the Mie theory.[27] The spectral dependence of the scattering coefficient, according to the Mie theory is $\lambda^{-\eta}$, where λ is the wavelength and η is an exponent that is affected by the scatterers types (grains, pores) and their size, compared to the wavelength, as shown in Eq. (7). The value of η and its dependence on the wavelength can provide useful information about the scatterers type and size.

Based on Figure 9 and on Eq. (7), we calculated the value of the exponent η for the attenuation curve and for the scattering curve in the wavelength range of 4.5–5.5 μm and the results were $\eta = 2$ and $\eta = 2.3$, respectively.

We used the Mie theory to carry out numerical calculations of scattering by pores of different radii $\langle a \rangle$ inside the silver halide host at the wavelength $\lambda = 5\,\mu$m. These calculations yielded a correlation between η and the average radius

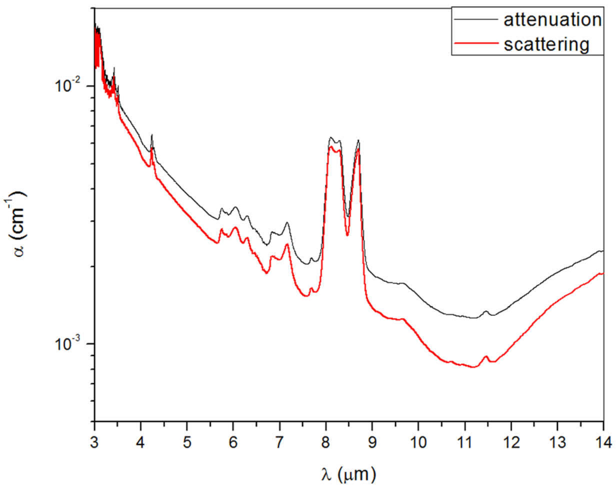

FIG. 9. The scattring coefficient curve compared to the atteuation coefficient curve in the mid-IR for $AgCl_{0.3}Br_{0.7}$ fiber.

of the pores. Using the correlation between η and $\langle a \rangle$, we were able to determine the average radius $\langle a \rangle$ of the pores. Based on the η value determined from the attenuation curve, $\langle a \rangle$ was found to be 0.7 μm, and based on the η value determined from the scattering curve, $\langle a \rangle$ was found to be 0.5 μm. Such an analysis will be more accurate if it will use the η value from the scattering curve, instead of the η value from the attenuation curve, especially if the scatterers are pores.[20]

VI. CONCLUSIONS

The spectral absorption of silver halide crystals, deformed crystals, and fibers extruded from these crystals and the attenuation of these fibers were measured in the mid-IR. The losses of the silver halide fibers were composed of absorption losses and scattering losses. By measuring both the total attenuation and the absorption of fibers in the mid-IR, we were able to determine the scattering coefficient. The spectral behavior of the absorption was compatible with the exponential low of a weak absorption tail. We therefore suggest that the weak absorption tail ascribed to defects, disorders, and impurities is responsible for the absorption below the known Urbach tail. We calculated the activation energy E_0 for the crystals, the deformed crystal, and extruded fibers for two compositions: $AgCl_{0.3}Br_{0.7}$ and AgBr, and showed that all values are in the same range of 0.3–0.5 eV. These values are compatible with the measurements done by other researches on other materials.[26] Analyzing the scattering, we determined the dependence of the power coefficient η on the wavelength. The η value, can be more accurate if it will be done on the scattering curve itself, calculated by subtracting the absorption measurements from the attenuation measurements.

The combined measurements of both the spectral total attenuation and the absorption allows a better understanding of the loss mechanisms in silver halide fibers in the infrared. We showed that most of the attenuation at the wavelength 10.6 μm is due to scattering losses. This points to the fact that most effort in improving silver halide fiber's transmission should be concentrated in reducing the scattering. Of course, the absorption will still be a limiting value even if the scattering will be lowered. A better understanding of the loss mechanisms in silver halide fibers, as shown in this work, will contribute to improved manufacturing processes and to the production of better transmitting fibers.

ACKNOWLEDGMENTS

The authors wish to thank Dr. L. Nagli and Dr. I. Shafir for fruitful discussions, and Mrs. I. Vasserman and Dr. G. Izakson for preparing the samples.

[1] J. A. Harrington, *Infrared Fibers and Their Applications* (SPIE Press, 2004).

[2] D. Bunimovich, L. Nagli, and A. Katzir, "Absorption measurements of mixed silver halide crystals and fibers by laser calorimetry," Appl. Opt. **33**(1), 117 (1994).

[3] D. Bunimovich, L. Nagli, Sh. Shalem, and A. Katzir, "Absorption spectrum of silver bromide crystals and fibers in the 9–11 μm wavelength range," J. Appl. Phys. **81**(3), 1612 (1997).

[4] L. Butvina, "Polycrystalline fibers," in *Infrared Fiber Optics*, edited by J. S. Sanghera and I. D. Aggarwal (CRC Press, 1998).

[5] L. N. Butvina and E. M. Dianov, "Optical absorption by free carriers in materials for IR fibers," Proc. SPIE **484**, 21 (1984).

[6] L. N. Butvina, E. M. Dianov, N. V. Lichkova, V. N. Zavgorodnev, and I. Kuepper, "Crystalline silver halide fibers with optical losses lower than 50 dB/km in broad IR region and their applications," Proc. SPIE **4083**, 238 (2000).

[7] L. N. Butvina, V. V. Vojtsekhovsky, E. M. Dianov, and A. M. Prokhorov, "Light scattering by voids in polycrystalline fibers," Proc. SPIE **843**, 105 (1987).

[8] A. Sa'ar and A. Katzir, "Scattering effects in crystalline infrared fibers," J. Opt. Soc. Am. A **5**(6), 823 (1988).

[9] S. Sliberstein, J. Kastner, M. Tacke, I. Schnitzer, and A. Katzir, "Propagation of infrared radiation in silver halide optical fibers," Proc. SPIE **2977**, 74 (1997).

[10] D. Bunimovich, S. Shalem, and A. Katzir, "Effects of thermal treatment on the infrared transmission of polycrystalline silver halide fibers," Appl. Opt. **36**(1), 285 (1997).

[11] A. Hordvik, "Measurements techniques for small absorption coefficients: Recent advances," Appl. Opt. **16**, 2827 (1977).

[12] V. G. Artyushenko, E. M. Dianov, and E. P. Nikitin, "Calorimetric method of determining the bulk and surface absorption in the infrared-transparent materials," Sov. J. Quantum Electron **8**, 608 (1978).

[13] H. B. Rosenstock, M. Hass, D. A. Gregory, and J. A. Harrington, "Analysis of laser calorimetric data," Appl. Opt. **16**, 2837 (1977).

[14] D. A. Pinnow and T. C. Rich, "Development of a calorimetric method for making precision optical absorption measurements," Appl. Opt. **12**, 984 (1973).

[15] L. C. Nistor, S. V. Nistor, V. Teodorescu, E. Cojocaru, and I. M. Mihailescu, "Calorimetric absorption coefficient measurements using pulsed CO_2 lasers," Appl. Opt. **18**, 3517 (1979).

[16] L. C. Nistor, S. V. Nistor, and V. Teodorescu, "High sensitivity apparatus for low optical absorption measurements," J. Appl. Phys. **56**, 6 (1984).

[17] Kh. S. Bagdasarov, V. I. Zhekov, T. M. Murina, A. V. Popv, A. M. Prokhorov, and E. A. Fedorov, "Pulse laser calorimetry," Sov. J. Quantum Electron. **18**(3), 415 (1988).

[18] V. I. Zhekov, T. M. Murina, A. V. Popv, and A. M. Prokhorov, "Nonlinear bulk absorption in $Y_{3-x}Er_xAl_5O_{12}$ crystals," JEPT Lett. **45**(6), 346 (1987), available at http://www.jetpletters.ac.ru/ps/1240/article_18747.shtml.

[19] R. Hui and M. O'Sullivan, *Fiber Optic Measurement Techniques* (Academic Press, 2008), p. 382.

[20] S. Israeli and A. Katzir, "Optical losses of AgClBr crystals and fibers in the middle infrared," Opt. Mater. **33**, 1825 (2011).

[21] P. J. Severin, "Calorimetric measurements of weakly absorbing materials: Theory," Appl. Opt. **18**(10), 1546 (1979).

[22] S. Israeli and A. Katzir, "Absorption measurements on silver bromide crystals and fibers in the infrared," J. Appl. Phys. **113**, 043111 (2013).

[23] F. Moser, D. Bunimovich, A. DeRowe, O. Eyal, A. German, Y. Gotshal, A. Levite, L. Nagli, A. Ravid, V. Scharf, S. Shalem, D. Shemesh, R. Simchi, I. Vasserman, and A. Katzir, "Medical applications of infrared transmitting silver halide fibers," IEEE J. Sel. Top. Quantum Electron **2**, 872 (1996).

[24] J. S. Sanghera, V. Q. Nguyen, P. C. Pureza, R. E. Miklos, F. H. Kung, and I. D. Aggarwal, "Fabrication of long lengths of low-loss IR transmitting $AS_{40}S_{(60-X)}$ Se_x glass fibers," J. Lightwave Technol. **14**(5), 743 (1996).

[25] W. J. Chung, B. J. Park, H. S. Seo, J. T. Ahn, M. H. Lee, and Y. G. Choi, "Effects of the weak absorption tail on the transmission loss of Ge–Sb–Se optical fibers," J. Am. Ceram. Soc. **88**(5), 1205(2005).

[26] M. Hidefumi and I. Tatsuo, "A new loss mechanism in ultralow loss optical materials," J. Appl. Phys. **51**(4), 2270 (1980).

[27] C. F. Bohren and D. R. Huffman, *Absorption and Scattering of Light by Small Particles* (Wiley, New York, 1983).